BULLETIN OF THE CHEMICAL SOCIETY OF JAPAN, VOL. 45, 2259—2265 (1972)

Magnetic Susceptibilities and Broad-Line PMR Spectra of Dichloro(pyridazine)copper(II) and Related Compounds

Shuji Emori, Motomichi Inoue, and Masaji Kubo
Department of Chemistry, Nagoya University, Chikusa, Nagoya

(Received February 14, 1972)

The magnetic susceptibilities of CuX_2L (X: halide ion, L: 1,2,4-triazole, pyridazine, phthalazine, 4-amino-1,2,4-triazole) conform to the linear Ising model or Heisenberg model, indicating the presence of linear magnetic chains in the crystals. Fermi contact shift observed in the broad-line PMR spectrum indicates the diffusion of a positive hole from a copper atom to the molecule of heterocycles. The magnitude of the exchange integrals is related to the spin densities on the atoms of the heterocycles.

In the crystals of dichloro(1,2,4-triazole)copper(II), $CuCl_2$(tr), each copper atoms has a distorted octahedral coordination of four chlorine atoms and two nitrogen atoms.[1] The octahedra are joined with one another by sharing chlorine edges and are also linked by 1,2,4-triazole molecules, constituting an infinite linear chain as the structural unit. The magnetic susceptibility of the compound conforms to the linear Ising model.[2] From contact shifts in PMR spectrum, spin densities on atoms in 1,2,4-triazole have been evaluated.[3] From these, it was concluded that superexchange interaction operates between copper atoms through the heterocycle. From the same steric reason as for 1,2,4-triazole in $CuCl_2$(tr), a bidentate heterocyclic ligand having two neighboring nitrogen atoms (for example, pyridazine and phthalazine) is expected to coordinate to two copper atoms.[4] Therefore, in the crystals of CuX_2L type complexes (X: halide ion, L: bidentate nitrogen heterocycle), the magnetic unit is presumed to be an infinite linear chain, –Cu–L–Cu—, analogous to that in $CuCl_2$(tr). In this linear chain, superexchange

1) J. A. J. Jarvis, *Acta. Crystallogr.*, **15** 964 (1962).
2) M. Inoue, S. Emori, and M. Kubo, *Inorg. Chem.*, **7**, 1427 (1968).
3) M. Inoue and M. Kubo, *ibid.*, **5**, 70 (1966).
4) K. Hyde, G. F. Kokozska, and G. Gordon, *J. Inorg. Nucl. Chem.*, **31**, 1993 (1969).

interaction can operate between copper atoms through the molecules of the heterocycles, its magnitude depending on the electronic state of bridging ligands.[5] Therefore, we have measured the magnetic susceptibilities of this type of complexes in order to estimate exchange integrals and also recorded broad-line PMR spectra to evaluate the spin densities on atoms in the heterocycles.

Experimental

$CuCl_2L$ was prepared by modifying the method of Hyde *et al.*[4] A solution of an appropriate nitrogen heterocycle in 1 N hydrochloric acid was added in slight excess to a solution of copper(II) chloride in 3 N hydrochloric acid. On standing, green powder crystals separated. They were recrystallized from 3 N hydrochloric acid. $CuBr_2L$ was prepared in the same manner as for $CuCl_2L$ using hydrobromic acid in place of hydrochloric acid. The results of chemical analysis are listed in Table 1.

Table 1. Analytical data for CuX_2L

Compound		Cu, %	C, %	H, %	N, %	Cl or Br %
$CuCl_2$(pid)	Found	29.34	21.71	1.58	12.89	33.02
	Calcd	29.62	22.39	1.88	13.06	33.05
$CuCl_2$(pht)	Found	24.21	36.19	1.96	10.54	26.89
	Calcd	24.02	36.31	2.29	10.59	26.80
$CuCl_2$(atr)	Found	29.11	10.91	1.55	25.85	32.41
	Calcd	29.08	10.99	1.85	25.64	32.44
$CuBr_2$(tr)	Found	21.76	8.22	0.85	14.34	54.51
	Calcd	21.73	8.21	1.04	14.37	54.64
$CuBr_2$(pid)	Found	20.79	15.84	1.17	9.18	52.15
	Calcd	20.94	15.83	1.33	9.23	52.67
$CuBr_2$(pht)	Found	17.81	27.07	1.53	7.77	44.33
	Calcd	17.98	27.18	1.71	7.92	45.21
$CuBr_2$(atr)	Found	20.61	7.82	1.13	17.98	51.86
	Calcd	20.67	7.81	1.31	18.23	51.98

pid: pyridazine, pht: phthalazine, tr: 1,2,4-triazole, atr: 4-amino-1,2,4-triazole.

Magnetic susceptibility was determined by means of magnetic balances described in our previous paper.[2] The molar susceptibilities were corrected for diamagnetic contributions (in 10^{-6} emu/mol) from copper ions (−11),[6] chloride ions (−26),[6] bromide ions (−36),[6] 1,2,4-triazole (−38),[7] pyridazine (−38), phthalazine (−75), and 4-amino-1,2,4-triazole (−46). The value for pyridazine was assumed to be equal to that of pyrazine.[7] The values for phthalazine and 4-amino-1,2,4-triazole were evaluated on the basis of those for pyridazine and 1,2,4-triazole, respectively, by use of the Pascal constants. The temperature-independent paramagnetism was assumed to be equal to 60×10^{-6} emu/mol.[8]

The PMR spectra of the powder crystals were recorded at 25°C by means of a Model JNS-B broad-line NMR spectrometer from JEOLCO operating at 29.7 MHz with an amplitude of magnetic field modulation equal to 1.0 Oe. Water was employed as an external standard.

Results

The susceptibilities corrected for diamagnetic contributions and the temperature-independent paramagnetism obey the Curie-Weiss law at high temperatures as shown in Fig. 1. The Weiss constants and g-values evaluated from the Curie constants are listed in Table 2. The susceptibilities in the low-temperature region are plotted against the temper-

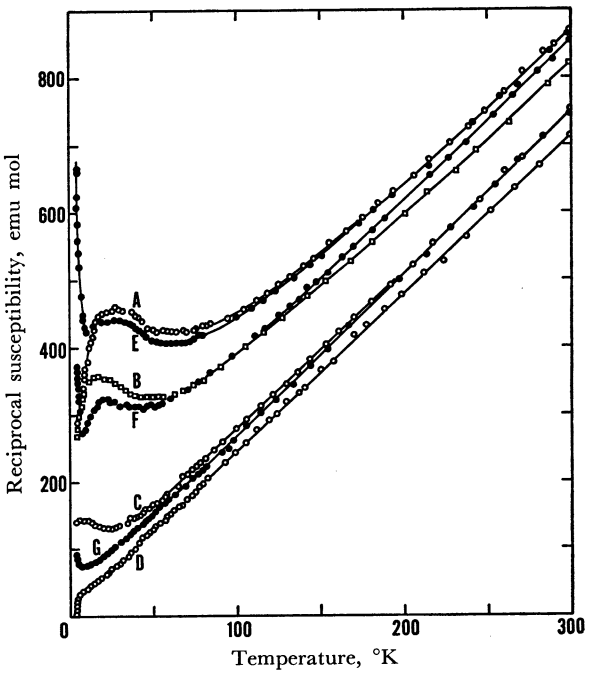

Fig. 1. Reciprocal susceptibilities of $CuCl_2$(pid) (A), $CuCl_2$(pht) (B), $CuCl_2$(atr) (C), $CuBr_2$(tr) (D), $CuBr_2$(pid) (E), $CuBr_2$(pht) (F), and $CuBr_2$(atr) (G) plotted against the temperature.

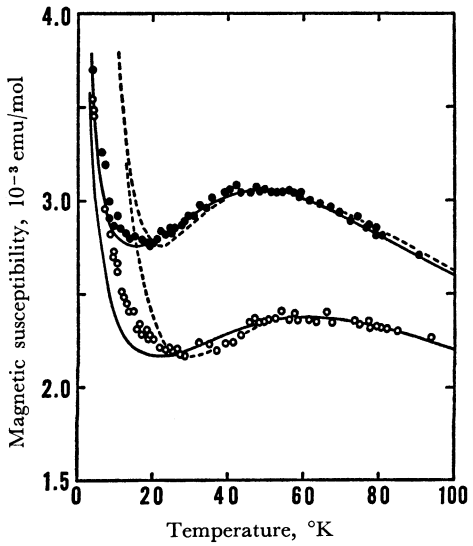

Fig. 2. Magnetic susceptibilities of $CuCl_2$(pid) (white circles) and $CuCl_2$(pht) (black circles). Solid curves: linear Heisenberg model. Broken curves: linear Ising model.

5) M. Inoue and M. Kubo, *Inorg. Chem.*, **9**, 2310 (1970).
6) P. W. Selwood, "Magnetochemistry," 2nd ed., Interscience Publishers, New York, N. Y. (1956), p. 78.
7) G. Foëx, "Constantes Sélectionées, Diamagnétisme et Paramagnétisme," Masson, Paris (1957).
8) B. N. Figgis and R. L. Martin, *J. Chem. Soc.*, **1956**, 3837.

Table 2. Weiss constant, θ, g-value evaluated from the Curie constant, g_C, and parameters, J/k, g, C_{low}, based on the Heisenberg model and the Ising model

Compound	θ, °K	g_C	Heisenberg model			Ising model		
			J/k, °K	g	C_{low}	J/k, °K	g	C_{low}
$CuCl_2$(tr)[a]	−19.0	2.13	—	—	—[b]	−17.9	2.07	0.027[d]
$CuCl_2$(pid)	−61.5	2.10	−51.7	2.06	0.000135	−87.3	2.13	0.000478
$CuCl_2$(pht)	−61.2	2.17	−40.6	2.08	0.000151	−68.0	2.16	0.000603
$CuCl_2$(atr)	−18.3	2.13	−17.6	2.17	0.000377	−29.4	2.26	0.00153
$CuBr_2$(tr)	−6.7	2.13	—	—	—[b]	−8.3	2.10	0.046[e]
$CuBr_2$(pid)	−69.0	2.13	−45.8	1.98	0.000129	−76.4	2.05	0.000492
$CuBr_2$(pht)	−47.4	2.08	−36.0	1.98	0.000274	−63.4	2.09	0.000714
$CuBr_2$(atr)	−10.1	2.10	−7.58	1.93	—[c]	−9.36	1.92	—[c]

a) Ref. 2. b) The Heisenberg model does not give good agreement with experimental data. c) No paramagnetic behavior was observed at low temperature. d) $\theta_{low}=2.5$°K. e) $\theta_{low}=2.8$°K.

ature in Figs. 2—6.

The observed PMR absorption derivative curves are shown in Figs. 7—10. Dibromo(1,2,4-triazole)-copper(II), $CuBr_2$(tr), dichloro(pyridazine)copper-(II), $CuCl_2$(pid), dibromo(pyridazine)copper(II), $CuBr_2$(pid), and dibromo(phthalazine)copper(II), $CuBr_2$(pht), show asymmetric curves, each of which can be decomposed into two simple derivative curves, one shifted to the low-field side and the other shifted to the high-field side. The shifts, $\Delta H/H$, are listed in Table 3. The curve of dichloro(phthalazine)copper-(II), $CuCl_2$(pht), is made up of a broad component

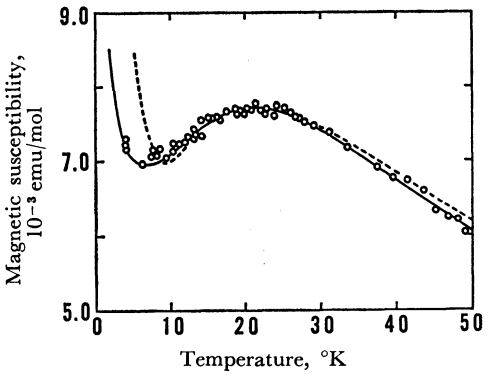

Fig. 3. Magnetic susceptibility of $CuCl_2$(atr). Solid curve: linear Heisenberg model. Broken curves: linear Ising model.

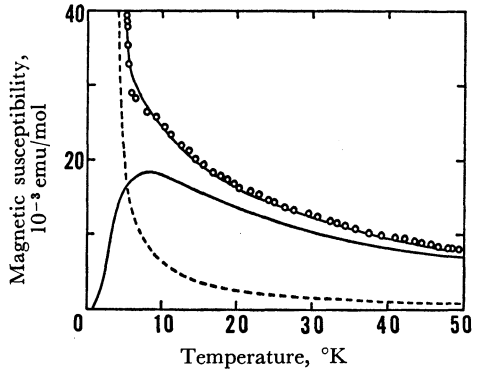

Fig. 4. Magnetic susceptibility of $CuBr_2$(tr) resolved into a low-temperature Curie-Weiss curve (broken curve) and a curve for the linear Ising model.

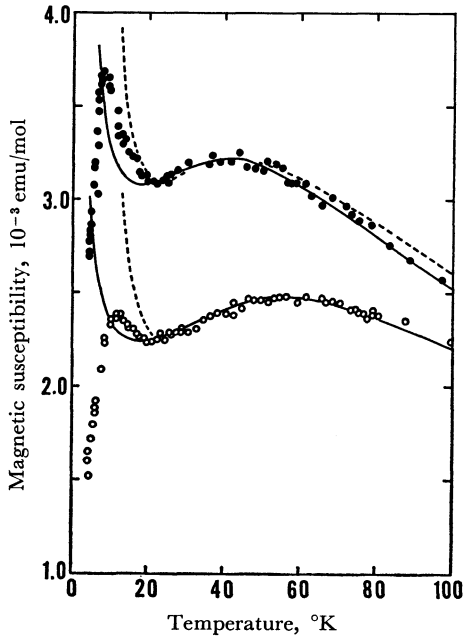

Fig. 5. Magnetic susceptibilities of $CuBr_2$(pid) (white circles) and $CuBr_2$(pht) (black circles). Solid curves: linear Heisenberg model. Broken curves: linear Ising model.

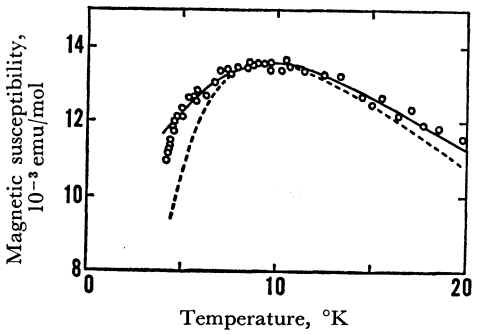

Fig. 6. Magnetic susceptibility of $CuBr_2$(atr). Solid curve: linear Heisenberg model. Broken curve: linear Ising model.

having a low-field shift, another broad component having a high-field shift, and a sharp component. The integrated intensity of the sharp component amounted to less than 0.1% of the total intensity and fluctuated among different preparations. Therefore,

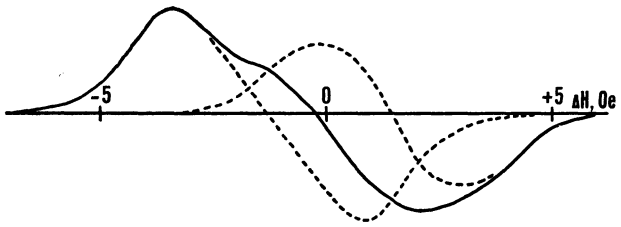

Fig. 7. PMR absorption derivative curve (full curve) of $CuBr_2(tr)$ decomposed into two simple derivative curves (broken curves).

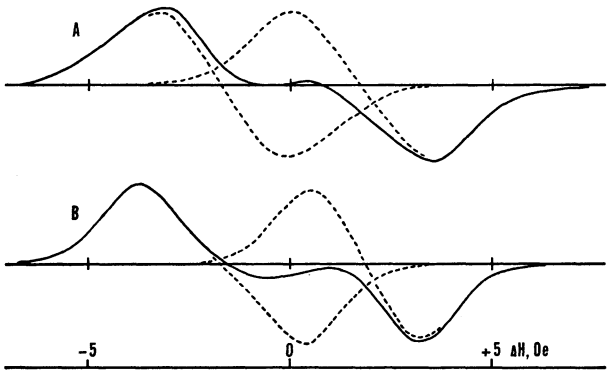

Fig. 8. PMR absorption derivative curves of $CuCl_2(pid)$ (A) and $CuBr_2(pid)$ (B). Each curve (full curve) is decomposed into two simple derivative curves (broken curves).

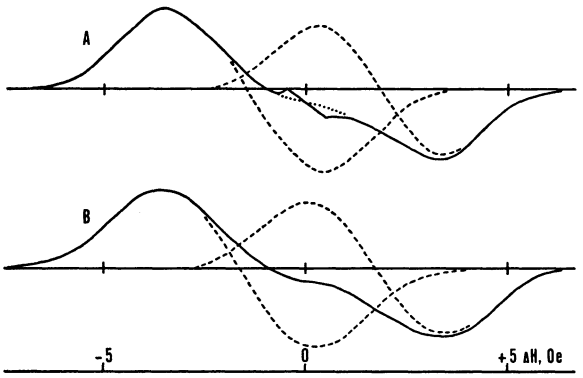

Fig. 9. PMR absorption derivative curves (full curves) of $CuCl_2(pht)$ (A) and $CuBr_2(pht)$ (B). The dotted curve in (A) shows the superposition of two derivative curves. A sharp unshifted component appears. The intrinsic absorption derivative curve of each compound is decomposed into two simple derivative curves(broken curves).

the unshifted curve is attributable to impurities or protons in randomly tumbling molecules. The dotted curve in Fig. 9A shows the superposition of the two broad curves and agrees with the observed curve except for a region near the unshifted component. The PMR absorption curves of dichloro(4-amino-1,2,4-triazole)copper(II), $CuCl_2(atr)$, and dibromo-(4-amino-1,2,4-triazole)copper(II), $CuBr_2(atr)$, also yield a sharp unshifted component, the integrated intensity of which is less than 1% and 0.5% of the total intensity, respectively. The intrinsic absorption curve of each of these compounds can be decomposed into two components.

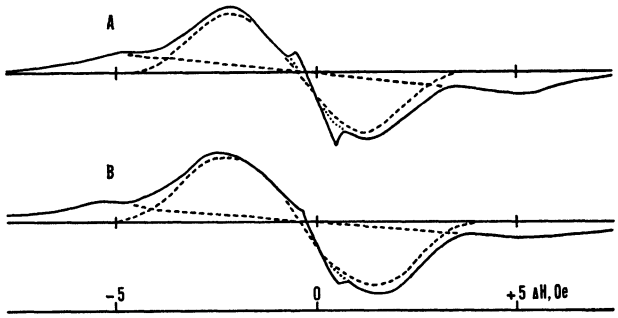

Fig. 10. PMR absorption derivative curves (full curves) of $CuCl_2(atr)$ (A) and $CuBr_2(atr)$ (B). Each of the dotted curves represent the superposition of two derivative curves (broken curves). In addition, a sharp component appears near the origin.

Table 3. Contact shift, $\Delta H/H$, contact interaction constant, a_i, and spin density, ρ_i

Compound	$\Delta H/H$ $\times 10^4$	Relative intensity	a_i, Oe	ρ_i
$CuCl_2(tr)$[a]	−1.3	2(3,5-CH)	+1.8	−0.08
	+1.4	1(4-NH)	−1.9	+0.06
$CuCl_2(pid)$	−2.5	1(3,6-CH)	+3.9	−0.16
	+2.5	1(4,5-CH)	−3.9	+0.16
$CuCl_2(pht)$	−2.1	2(1,4,5,8-CH)	+3.1	−0.13
	+2.6	1(6,7-CH)	−3.9	+0.16
$CuCl_2(atr)$	−0.7	(3,5-CH)	+0.9	−0.04
	—[b]	($N-NH_2$)	+	+
$CuBr_2(tr)$	−1.9	2(3,5-CH)	+2.5	−0.11
	+2.1	1(4-NH)	−2.7	+0.08
$CuBr_2(pid)$	−2.5	1(3,6-CH)	+3.9	−0.16
	+2.7	1(4,5-CH)	−4.2	+0.18
$CuBr_2(pht)$	−2.4	2(1,4,5,8-CH)	+3.6	−0.15
	+2.5	1(6,7-CH)	−3.8	+0.16
$CuBr_2(atr)$	−0.6	(3,5-CH)	+0.8	−0.03
	—[b]	($N-NH_2$)	+	+

a) In ref. 3, a_i and ρ_i were evaluated assuming $g=2.00$. The values in this table are based on g_C. b) The absolute value could not be determined.

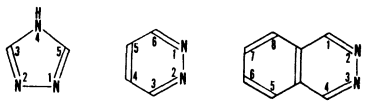

Discussion

The susceptibility *versus* temperature curve observed for $CuCl_2(pid)$ exhibits a broad maximum at about 60°K and a paramagnetic behavior below about 20°K as shown in Fig. 2. $CuCl_2(pht)$ and $CuCl_2$-(atr) shows a magnetic behavior resembling that of $CuCl_2(pid)$ (Figs. 2 and 3). These magnetic properties are characteristic of linear antiferromagnets, typical examples of which are $CuCl_2(tr)$,[2] potassium trifluorocuprate(II),[9] and 2,5-dihydroxy-*p*-benzoquinonatocopper(II).[10]

The susceptibility of $CuCl_2(tr)$ has already been determined between 4.2 and 300°K (Fig. 3 in Ref. 2). With decreasing temperature, the susceptibility passes

through a maximum at about 11°K and increases sharply obeying the Curie-Weiss law below about 8°K. The behavior below 8°K is due either to the effect of magnetically isolated copper(II) ions existent in a small quantity or to interaction between linear chains. Susceptibility attributable to these effects was subtracted from the observed values. The resulting intrinsic susceptibility conforms to the parallel susceptibility, χ, of a linear Ising chain.[11]

$$\chi = \frac{Ng^2\beta^2}{4kT} \exp \frac{J}{kT} \quad (1)$$

Here apart from obvious notations, J denotes the exchange integral between the nearest neighbors in a chain. Therefore, the susceptibility of $CuCl_2$(tr) can be expressed by

$$\chi = \frac{Ng^2\beta^2}{4kT} \exp \frac{J}{kT} + \frac{C_{low}}{T-\theta_{low}} \quad (2)$$

where C_{low} and θ_{low} are the Curie constant and the Weiss constant in the low temperature region, respectively. From the susceptibility of $CuCl_2$(pid), C_{low} and θ_{low} cannot be determined accurately, because the temperature range of the paramagnetic effect is narrow. However, θ_{low} is estimated to be almost equal to 0°K (see Fig. 1). Therefore, the value of θ_{low} was assumed to be 0°K and g, J, and C_{low} were varied to get the best fit to the observed susceptibility especially near the temperature of the maximum susceptibility. The broken curve in Fig. 2 shows the result of calculation carried out with parameters listed in Table 2. Fisher[12] has pointed out that the perpendicular susceptibility given by

$$\chi = \frac{Ng^2\beta^2}{4|J|}\left[\tanh \frac{|J|}{2kT} + \frac{|J|}{2kT} \operatorname{sech}^2 \frac{|J|}{2kT}\right] \quad (3)$$

should be taken into account as well in the linear Ising model. However, all attempts to calculate curves involving both parallel and perpendicular components failed to reproduce the observed relative susceptibility as well as the absolute susceptibility. Bonner and Fisher[13] have calculated the susceptibility of a one-dimensional Heisenberg spin lattice. The observed susceptibility agrees well with the Bonner-Fisher curve corrected for the paramagnetic behavior in the low temperature region (see Fig. 2). For $CuCl_2$(pht) and $CuCl_2$(atr), the exchange integrals and the g-values were evaluated by the same procedure as employed for $CuCl_2$(pid) (see Table 2 and Figs. 2 and 3). The g-values are almost equal to those evaluated from the Curie constants and also to a value, 2.13±0.03, determined by ESR[4] (see Table 2). These support a presumption that –Cu–L–Cu— chains are formed in the crystals of the chlorine compounds. Hyde *et al.*[4] have carried out an ESR measurement on $CuCl_2$(pid) and suggested that the Heisenberg model rather than the Ising model is adequate because the value of $|D/J|$ is very small (D is the dipole-dipole interaction constant for spins in an axially symmetric crystal field). In fact, the observed susceptibility agrees with the theoretical curve for the Heisenberg model more closely than that for the Ising model.

The crystal of $CuBr_2$(tr) is expected to be isostructural with $CuCl_2$(tr). The susceptibility *versus* temperature curve can be reproduced by Eq. 2 in a manner similar to the case of $CuCl_2$(tr) (see Table 2 and Fig. 4). However, the Heisenberg model gives poor agreement with experimental data as in the case of $CuCl_2$(tr).[2]

The susceptibility *versus* temperature curve observed for $CuBr_2$(pid) exhibits two maxima at 12 and 55°K (see Fig. 5). The broad maximum at the higher temperature is undoubtedly due to a short-range magnetic interaction within a linear chain. Another maximum at the lower temperature is attributable to a three-dimensional long-range ordering existing below the temperature owing to interaction between chains.[14] The magnetic behavior of $CuBr_2$(pht) resembles that of $CuBr_2$(pid) as shown in Fig. 5. The susceptibilities of $CuBr_2$(pid) and $CuBr_2$(pht) at high temperature can be analyzed in the same way as for $CuCl_2$(pid). The g-values obtained from the Ising model are nearly equal to those evaluated from the Curie constants (see Table 2). On the other hand, the g-values based on the Heisenberg model are smaller than 2.00, whereas the g-value of a copper ion should be greater than 2.00 owing to spin-orbit interaction. This inconsistency indicates that the susceptibilities calculated with the Heisenberg model can hardly be fitted to the observed absolute susceptibilities despite an apparent qualitative agreement as in Fig. 5. Presumably this discrepancy is due to a strong magnetic interaction between chains suggested by the appearance of two maxima in the susceptibility *versus* temperature curves. The susceptibility of $CuBr_2$(atr) can be explained with difficulty by the Ising model as well as by the Heisenberg model (see Table 2 and Fig. 6) presumably because interaction exists between chains. A coupled-double-chain model[15,16] gives an approximation to the susceptibility of a crystal consisting of infinite chains, each of which is weakly coupled with neighboring chains. However, curves calculated with this model fail to agree with the observed susceptibility. Table 2 lists exchange integrals evaluated on the basis of the Heisenberg and Ising models for an isolated linear chain. The $J/\mathbf{k}$ values of the bromine compounds have some significance for the comparison of exchange interaction among the compounds. The effect of magnetic interaction between chains appears markedly in the bromine compounds, suggesting that the interaction takes place through bromine atoms.

An asymmetric PMR absorption curve observed for

9) S. Kadota, I. Yamada, S. Yoneyama, and K. Hirakawa, *J. Phys. Soc. Japan*, **23**, 751 (1967).
10) H. Kobayashi, T. Haseda, E. Kanda, and S. Kanda, *ibid.*, **18**, 349 (1963).
11) G. F. Newell and E. W. Montroll, *Rev. Mod. Phys.*, **25**, 353 (1953).
12) M. E. Fisher, *J. Math. Phys.*, **4**, 124 (1963).
13) J. C. Bonner and M. E. Fisher, *Phys. Rev.*, **135**, A640 (1964).
14) S. Emori, M. Inoue, and M. Kubo, *Inorg. Chem.*, **8**, 1385 (1969).
15) M. Inoue and M. Kubo, *J. Mag. Resonance*, **4**, 175 (1971).
16) S. Emori, M. Inoue, and M. Kubo, *This Bulletin*, **44**, 3299 (1971).

$CuBr_2$(tr) bears a striking resemblance to that of $CuCl_2$(tr) (see Fig. 7). This supports a presumption that $CuBr_2$(tr) is isostructural with $CuCl_2$(tr) and that all 1,2,4-triazole molecules are equivalent in the crystals.[1] From the intensity ratio, 2 : 1, of the two components, the stronger one on the low-field side is assigned to protons, 3-CH and 5-CH, bonded to carbon at positions 3 and 5, while the curve shifted to the high-field side is attributable to a proton, 4-NH, bonded to nitrogen at position 4. Undoubtedly, the shifts are due to the isotropic contact hyperfine interaction field and are given by[5,17]

$$\frac{\Delta H}{H} = -a_i\left(\frac{\gamma_e}{\gamma_N}\right)\frac{\chi}{g\beta N} \tag{4}$$

where H is the NMR field, a_i is the contact interaction constant of a proton bonded to carbon or nitrogen at position i, γ_e is the magnetogyric ratio of an electron, and γ_N is that of a nucleus. The constants, a_i, listed in Table 3 were calculated from the observed shifts, $\Delta H/H$, the susceptibility at room temperature, and the g-value evaluated from the Curie constant. For an aromatic radical species, in which spin density localized on the pπ orbital of a carbon atom interacts with a proton bonded to the carbon atom, a_i is related to the spin density, ρ_i, on the adjacent carbon atom by the McConnell relation:[17,18]

$$a_i = Q_{CH}\rho_i \tag{5}$$

where Q_{CH} is a proportionality constant, the value of which has been determined empirically as -22.5 Oe. This relation is expected to hold for protons bonded to nitrogen as well.[19] However, few data are available for Q_{NH}. Barton and Fraenkel[20] have carried out an ESR experiments on dihydropyrazine cation radicals and found that $Q_{NH}=-33.7$ Oe by use of $Q_{CH}=-23.7$ Oe. The values of Q_{CH} and Q_{NH} may vary to a considerable extent among different bonding types.[19] Using Barton and Fraenkel's values, we evaluated spin densities, $\rho_{3,5}$ and ρ_4 as listed in Table 3. Negative and positive spin densities are distributed alternately on atoms in a triazole ring: $\rho_{3,5}<0$ and $\rho_4>0$. The alternation in sign of the spin density indicates that ρ_1 and ρ_2 are positive. Accordingly, it is concluded that the migration of an unpaired electron from copper creates a positive spin density on nitrogen atoms bonded to copper.

For $CuCl_2$(pid), a_i and ρ_i were evaluated in the same manner as for $CuBr_2$(tr) and are listed in Table 3. In the crystals of $CuCl_2$(pid), all pyridazine molecules are presumed to be equivalent, because the crystal consists of linear chains, –Cu–(pid)–Cu–, as units. Hence, there are two kinds of protons in equal amounts in agreement with the result of PMR absorption. Since a positive spin density is expected to exist on nitrogen atoms bonded to copper as in CuX_2(tr), carbon atoms at positions 3 and 6 bear a negative spin density (see Table 2). Therefore, the absorption curve on the low-field side is attributable to protons, 3-CH and 6-CH, whereas the curve shifted to the high-field side is assigned to 4,5-CH protons, indicating that ρ_4 and ρ_5 are positive. For pyridazine anion radicals, the interaction constants, a_i, have been determined as $|a_{3,6}|=0.16$ Oe and $|a_{4,5}|=6.45$ Oe by ESR measurements.[21] A molecular-orbital calculation on the radical has shown that $a_{3,6}$ is positive whereas $a_{4,5}$ is negative (therefore, $\rho_{3,6}<0$ and $\rho_{4,5}>0$)[22] in support of our assignment. The ratio, $|a_{3,6}/a_{4,5}|=1.0$, for $CuCl_2$(pid) is much greater than 0.025 for a pyridazine anion radical. An odd electron in the radical is attracted to nitrogen owing to the difference between the electronegativities of carbon and nitrogen. Accordingly negative spin densities are induced on carbon atoms bonded to nitrogen. On the other hand, in the copper(II) complex positive spins are mostly localized on nitrogen atoms bonded to copper, because unpaired electrons migrate from copper to the molecules of the heterocycle. In π-bond conjugation, negative spin density on an atom increases with increasing positive spin density on adjacent atoms. This is the reason why the ratio, $|a_{3,6}/a_{4,5}|$, is larger in the copper complex than in the radical.

The observed absorption curve of $CuCl_2$(pht) can be decomposed into two simple curves of intensity ratio equal to 2 : 1 (see Fig. 9). In $CuCl_2$(pht), ρ_1 and ρ_4 are expected to be negative for the same reason as in $CuCl_2$(pid). In addition, an assumption of alternation in sign of the spin density leads to a conclusion that $\rho_{5,8}<0$ and $\rho_{6,7}>0$. These conform to the intensity ratio and the shifts of the two components (see Table 3). Although $\rho_{1,4}$ and $\rho_{5,8}$ must differ from each other, the stronger curve on the low-field side is difficult to resolve owing almost complete overlap. Table 3 gives average values. A molecular-orbital calculation carried out on a phthalazine anion radical has indicated the absence of a negative spin density on any carbon atoms.[22] However, in $CuCl_2$(pht), an unpaired electron migrating from copper gives rise to a strong polarization in the π-bond system of the heterocyclic ligand. Owing to this effect, negative spin densities are distributed on carbon atoms at positions, 1, 4, 5, and 8.

The intrinsic absorption curve of $CuCl_2$(atr) consists of a curve with a peak-to-peak width of 3.3 Oe and a broad curve with a width of 10 Oe (see Fig. 10). The narrower one can be assigned to protons, 3,5-CH, by comparing the curves with those of CuX_2(tr). Therefore, the broad curve is attributable to protons in N-NH_2. The shift, $\Delta H/H$, of the broad curve cannot be determined accurately because the curve is very broad and an absorption curve due to impurities is superposed on it. The shift, however, suggests that the nitrogen atom at position 4 carries a positive spin density, in conformity with the results of CuX_2(tr).

17) H. M. McConnell and D. B. Chesnut, *J. Chem. Phys.*, **28**, 107 (1958).
18) T. H. Brown, D. H. Anderson, and H. S. Gutowsky, *ibid.*, **33**, 720 (1960).
19) J. R. Bolton, "Radical Ions," ed. by E. T. Kaiser and L. Kevan, John Wiley & Sons, New York, N. Y. (1968), p. 19.
20) B. L. Barton and G. K. Fraenkel, *J. Chem. Phys.*, **41**, 1455 (1964).
21) E. W. Stone and A. H. Maki, *ibid.*, **39**, 1635 (1963).
22) J. A. Pople and D. L. Beveridge, "Approximate Molecular Orbital Theory," McGraw Hill, New York, N. Y. (1970), p. 134.

For $CuBr_2$(pid), $CuBr_2$(pht), and $CuBr_2$(atr), the spin densities can be evaluated in a manner similar to that for the corresponding chlorine compounds (see Table 3).

The magnitude of the exchange integrals depends on the kind of heterocycles rather than halide ions (see Table 2). This indicates the predominance of superexchange interaction through the heterocycles. CuX_2(pid) and CuX_2(pht) carry larger spin densities on the atoms of the heterocycles than do CuX_2(tr) and CuX_2(atr). Large spin densities on the atoms of bridging ligands favor the migration of positive holes and, consequently, superexchange interaction between copper atoms. In conformity with this expectation, the exchange integrals of CuX_2(pid) and CuX_2(pht) are greater than those of CuX_2(tr) and CuX_2(atr).

Our grateful thanks are due to Dr. M. Iwasaki and Dr. B. Eda of the Government Industrial Research Institute, Nagoya, for giving us facilities to use a broad-line NMR spectrometer in the Institute.